IET Networks

Special Issue: Advances in Internet of Things for Healthcare Systems

Wearable indoor localisation approach in Internet of Things

ISSN 2047-4954
Received on 31st January 2016
Revised on 30th May 2016
Accepted on 18th July 2016
doi: 10.1049/iet-net.2016.0007
www.ietdl.org

Haojun Huang[1], Jianguo Zhou[1] ✉, Wei Li[1], Juanbao Zhang[2], Xu Zhang[3], Guolin Hou[4]

[1]*School of Electronic Information, Wuhan University, Wuhan, People's Republic of China*
[2]*School of Computer Science and Technology, Zhongyuan University of Technology, Zhengzhou, People's Republic of China*
[3]*Department of Computer Science and Technology, Tsinghua University, Beijing, People's Republic of China*
[4]*Science and Technology on Near-surface Detection Laboratory, Wuxi, People's Republic of China*
✉ *E-mail: zjg@whu.edu.cn*

Abstract: Localisation is an essential and important research issue in Internet of Things (IoT). Most localisation schemes focus on outdoor IoT. However, indoor IoT is required in some applications such as target detection and tracking, and emerging smarter healthcare. As such, localisation approaches designed for indoor IoT are necessary. Note that the smarter healthcare emerges at an unprecedented speed while few localisation schemes can be directly exploited for them with accuracy guarantee. In this study, the authors propose a wearable indoor localisation approach to improve the localisation accuracy of previous work. In this approach, the wearable devices embedded into person are used to realise their displacement vector in mobile environments, thus estimating their own locations. In addition, the authors propose a walking prediction mechanism to increase localisation accuracy. The real-world experiment results demonstrate that the proposed approach achieves lower localisation error in various moving speeds.

1 Introduction

Over the past decades, Internet of Things (IoT) has attracted many research efforts in a wide range of applications such as military operations, tracking systems, and animal environment monitoring. In these applications, many schemes for IoT require nodes to know their physical locations. Examples include those for target detection and tracking, smarter healthcare, search and rescue, and so on [1, 2]. In order to obtain the location of sensors, one simple and precise solution is that each node equips with Global Positioning System (GPS) device. Unfortunately, it is too expensive to realise and is useless indoors. Furthermore, most applications require coarse localisation accuracy. As such, a reasonable solution is that some nodes of sensor network should be equipped with a GPS device, while the others obtain their locations automatically by a localisation approach.

There are many localisation approaches proposed, including two categories: range-based and range-free [2]. The range-based localisation schemes depend on distance or angle between two nodes to calculate the locations of nodes while the range-free localisation schemes estimates the locations of nodes by network connectivity [3]. Those schemes have their own advantages and limitation as well. Range-based schemes can achieve higher localisation accuracy with some special hardware compared with range-free schemes [4]. Currently, these localisation approaches focus on outdoor LoT, and furthermore, are useless for some indoor applications [5, 6]. For example, when an old man unexpectedly falls while walking in door, the indoor alarm system needs to send alerts according to the mobile sensor attached to him. So far, there is a specific range-based approach designed for wearable indoor localisation in mobile environments with accuracy guarantee [7, 8].

To address this issue, in this paper, we propose a wearable indoor localisation approach called wearable indoor localisation approach (WILA) to improve the localisation accuracy of previous work. In the proposed approach, the wearable devices embedded into the body of a person are used to realise their displacement vector, thus estimating their own locations. In addition, we propose a walking prediction mechanism that predicts the moving direction of nodes to increase localisation accuracy.

The rest of this paper is organised as follows. We review the related work of localisation approaches in Section 2. In Section 3, we describe the design and realisation of our proposed scheme. The real-world experiment results are given in Section 4. Finally, Section 5 concludes the paper.

2 Related work

Over the last few decades, many localisation approaches for IoT including sensor networks have been proposed to provide location information [1–23]. Generally speaking, these schemes are of two categories: range-based and range-free.

Range-based schemes can provide a better accuracy by using the absolute distance [10–13]. There are a lot of work using RF receivers and transmitters based on a time-of-arrival based range measurement or received-signal-strength based range measurement for localisation. In order to communicate, these methods have the ability to use modulated signals and can use separate channels. However the proposed methods measure only range information. In [10], the Monte Carlo approach is used to provide a range-based approach. In [15], a real-time indoor positioning system is proposed with RFID Heron-bilateration location estimation and inertial-navigation location estimation, based on internal inertial measurement unit module. In [10], a target localisation algorithm is proposed based on time detection and a voting mechanism. When using six sensors, the average error was 60 cm in an area of 6 m^2. However, the performance of it will be exacerbated since it neglects that if there is high data traffic when events are detected. In [17], the TDOA extraction and adaptive fuzzy clustering based on acoustic sensor are used to realise node localisation. The acoustic range was about 152 m and the average error was around 1 m. The disadvantage of it is that the performance will exacerbate when there is high error value. In [23], any a normal node without location information can estimate its own locations by gathering the locations of location-aware anchor nodes and the one-hop normal nodes whose locations have been estimated from the anchor nodes. In [5], both acoustic signals and inertial sensors are used to estimate the sensor positions simultaneously. In [6], the customised services are provided to occupants, considering energy consumption in indoor localisation. In [8], a mobile device determines its position relative to a known reference with centimetre precision, based exclusively on the capture of acoustic signals emitted by controlled sources around it. In our approach, the wearable devices are equipped into the person for localisation in indoor. It is different with the current schemes in the following aspects. First, it works in mobile environments, especially designed for indoor localisation. Second, it can predict the displacement vectors of mobile person equipped with wearable devices, thus estimating their current locations in mobile environments.

Range-free schemes cannot provide the same accuracy as the range-based schemes. However, they are convenient to be used in the real-world situations due to the lack of additional hardware [1, 2, 19–22]. Their performance will be exacerbated if anisotropic factors exist. In [19], the triangles have been exploited to locate a node. The centre of all triangles is the location of a node. With the location information of their neighbours, the Bézier curves [20] are used to estimate the possible locations of nodes in distributed manners. Inspired by the observation that in an anisotropic network the hop count field propagated from an anchor exhibits multiple patterns, a pattern-driven localisation scheme in [22] has been propose for anisotropic networks.

3 WILA: design and implementation

In this section, we present the WILA design and its implementation in detail. WILA mainly consists of three parts: moving detection, walking step calculation and mobility prediction. The moving detection focuses on counting the number of walking step, while walking step emphasises the length of walking step. With such two parameters, WILA can obtain its displacement distance to and from its reference locations. The latter mainly highlights its moving direction prediction. By combining the displacement distance and moving direction, WILA can obtain its current locations. The details of WILA are as follows.

3.1 Moving detection

The walking distance of a person can be detected by the product of its walking step times the length of steps. Note that the various parts, including the arm, waist, legs and other sports, of a mobile person, will produce the same constant acceleration, therefore the waist of the person equip with a sensor for moving detection. Usually, when a person walks, his waists can produce three direction changes in the acceleration. These three direction changes, derived from the acceleration data are shown in Figs. 1–3.

From the curve of the acceleration data in three directions, it can be found that the accelerations of three directions have a similar certain periodicity. Furthermore, the accelerations of them follow the similar sine curve if the noise interference has been removed.

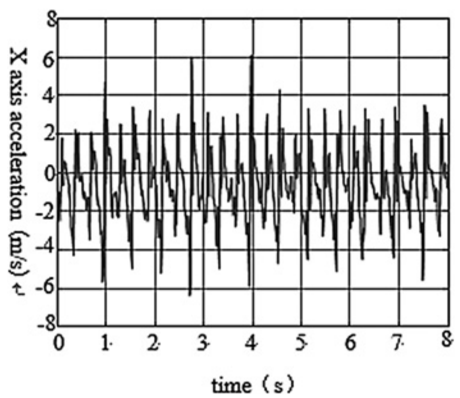

Fig. 1 *Acceleration direction in the X-axis when walking*

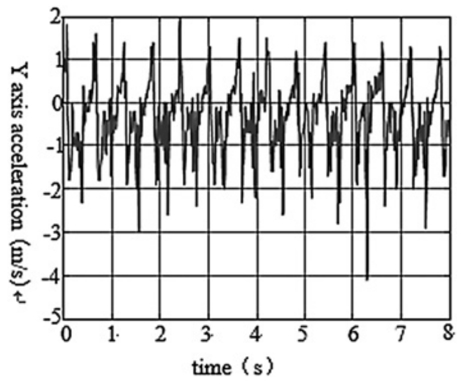

Fig. 2 *Acceleration direction in the Y-axis when walking*

Hence, we choose the acceleration of the Z-axis randomly to detect the counting the number of walking step.

Because the frequency of human walking is less than 5 Hz, the noise interference in our approach was removed by the low-pass finite impulse response (FIR) filter with the cutoff frequency of 5 Hz. The general form of the FIR filter can be expressed as

$$y(n) = \sum_{k=0}^{N-1} h(k)x(n-k) \qquad (1)$$

Where, $x(n)$ is the input signal, $y(n)$ is the output signal for the filter, N is the filter order, and $h(k)$ is the filter coefficient obtained from MATLAB [12]. Clearly, the higher the order of the filter, the better of the filtering effect. Furthermore, the current output time is related to the earlier time of the input. Therefore, we select several (e.g. 51) orders, and collect the data with a circular array in an efficient manner. The accelerations of Z-axis after it was filtered are shown in Fig. 4.

From Fig. 4, it can be seen that the acceleration curves exhibit the periodicity after filtering, and the value of each peak and trough of accelerations maps a step. Hence, we can know the steps of walking as long as all the peak and trough of the acceleration have been detected. It can not only remove the noise, but also cancel the frequency jitter by filtering, thus improving the accuracy of the detection step.

The simplest moving detection approach is to set a threshold, when the acceleration is greater than the threshold or lower than the threshold. Although this method is simple, it cannot obtain satisfactory results in all cases and is with poor robustness. The dynamic threshold with peak trough detection and time window are used to detect the moving, but with more complexes [10].

The test procedure is as follows:

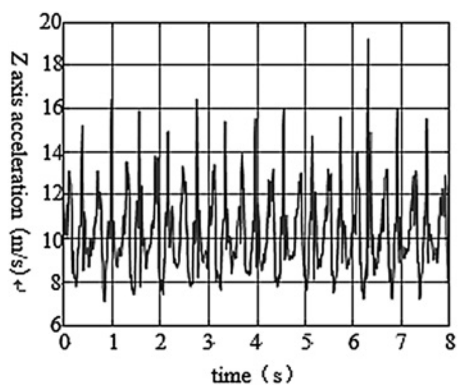

Fig. 3 *Acceleration direction in the Z-axis when walking*

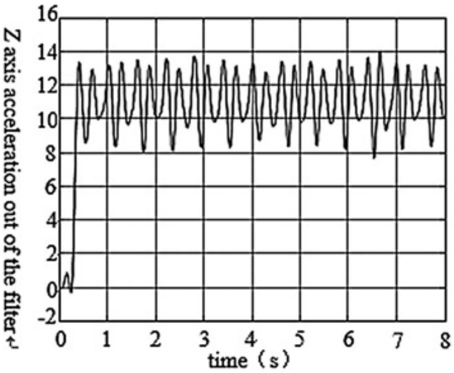

Fig. 4 *Acceleration of the Z-axis after filtering*

Step 1: Read the acceleration per 0.02 s, and send it into the low-pass filter, thus eliminating unwanted interference.
Step 2: Detect the peak of acceleration after pass through low-pass filtered to find a maximum value $A_{\max}$ and then to find a minimum value of $A_{\min}$. Otherwise, jump to step 1.
Step 3: Detection of peak trough, namely determine whether the difference between $A_{\max}$ and $A_{\min}$ is greater than a threshold.
Step 4: Output the efficient $A_{\max}$ and $A_{\min}$, and determine whether the person has been out.

The peak and trough of the acceleration curve are shown in Fig. 5. By using this method, we can obtain the same effect as the dynamic threshold and peak trough detection combine with time window.

3.2 Walking step calculation

The step size depends on the length of the legs and the walking speed. Note that there are up 40% of people who have differences in legs, we use the motion model of human walking to make the step size more accurate, as shown in Fig. 6. The legs are moving alternatively. Taking this step in Fig. 6 as example, people first lift the right foot, then the vertical acceleration begins to increase, the buttocks also begins to rise; when the left leg moves in the vertical direction, the buttocks reaches the highest point; finally, the acceleration decreases to the minimum when the right leg moves to the ground. The step length can be expressed as

$$\begin{aligned} \text{steplength} &= \frac{2 \times \text{vertical displacement}}{\tan \alpha} \\ &\simeq \frac{2 \times \text{vertical displacement}}{\alpha} \end{aligned} \tag{2}$$

Where, α is a very small angle, which can be considered as a constant value. In this paper, we use a simplified formula of AD [13] to

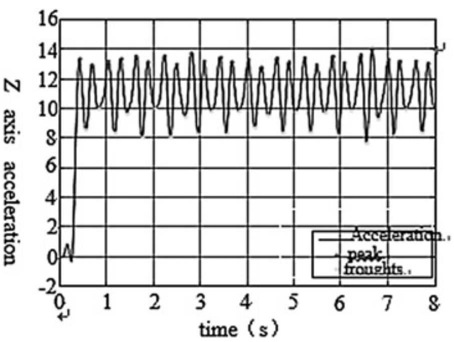

Fig. 5 *Peak and trough detection of acceleration*

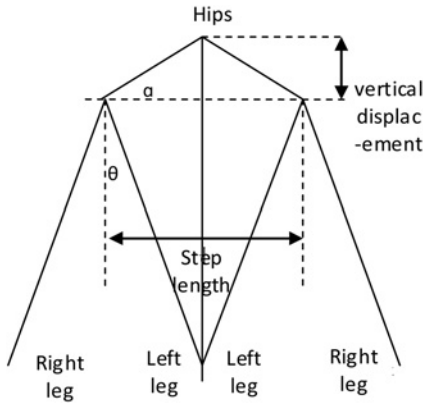

Fig. 6 *Schematic diagram of hip and leg movements when walking*

calculate the step size

$$\text{steplength} \simeq 4\sqrt{A_{\max} - A_{\min}} \times K \tag{3}$$

Where, $A_{\max}$ and $A_{\min}$ indicate the maximum and the minimum vertical accelerations in a single step, and K is a constant value for unit conversion.

To improve the accuracy of the step size, we use a varying K for different people, by training. The training method is to walk a certain distance L_r and record the output of the system l_0, and then the K value of the system k_r can be calculated as follows.

$$K_r = \frac{L_r}{L_0} \times K \tag{4}$$

3.3 Mobility prediction

Both gyroscope and magnetometer are good at detecting direction, but the magnetometer is used in navigation system due to its availability. The geomagnetic field is used to determine the absolute track of carrier in it, hence the error will not diverge over time while disturbancing by the surrounding environment. Once used in a mobile person, it will also cause measurement errors in the direction of walking due to mobility. Therefore, it is difficult to obtain high precision only with magnetometer. Fortunately, the gyroscope can work with it well due to its high precision. In order to facilitate understanding, we list the advantages and disadvantages of them in Table 1.

Since it takes long time to acquaint data from the gyroscope, the error accumulation cannot be avoided. Note it is close to 10° in experiments lasting for 100 s, so in our approach the Kalman filter is used to process the data. According to the principle of Kalman filter, the gyroscope data can be used to predict the walking direction, and then as measurement data originated from magnetometer gyroscope to correct it in real time, thus improving the accuracy of walking direction.

Let X_k be the walking direction of people, and U_k represent the angular velocity gyroscope output, Z_k be the heading angle from the calculation of magnetometer, i.e. X_k notes the state variable of

Table 1 Comparison of magnetometer and gyroscope

Measurement device	Advantage	Disadvantage
magnetometer	the errors of the absolute direction do not diverge in time	easily affected by the outside world
gyroscope	small outside interference high precision in short time	can only get the relative direction errors diverge versus time

IET Netw., 2016, Vol. 5, Iss. 5, pp. 122–126

Table 2 Test results of pedometer under different walking speed

Conner	Number	Walk step	Low speed	Normal speed	High speed
A	1	50	48	49	50
	2	50	49	50	50
B	1	50	50	50	50
	2	50	48	50	50
C	1	50	49	50	50
	2	50	49	50	50
D	1	50	49	50	50
	2	50	50	49	50
E	1	50	47	49	50
	2	50	49	50	50

the system, $Z_k$is the measured value of the system. Following to the principle of Kalman filter [14], we have

$$X_k = X_{k-1} + T_s U_k \tag{5}$$

Further, it can be expressed by

$$X_{k|k-1} = X_{k-1|k-1} + T_s U_k \tag{6}$$

$$P_{k|k-1} = P_{k-1|k-1} + Q \tag{7}$$

$$Kg = P_{k|k-1}/(P_{k|k-1} + R) \tag{8}$$

$$X_{k|k} = X_{k|k-1} + Kg(Z_k - X_{k|k-1}) \tag{9}$$

$$P_{k|k} = (1 - Kg)P_{k|k-1} \tag{10}$$

By this way, we can predict the walking direction of people. Since only the Kalman filter are used in one dimension, our system are more scale and efficient and suitable for the embedded system.

4 Simulation results

To evaluate the efficiency of our proposed WILA approach, we test the performance of our approach in the real-world experiments.

4.1 Step and displacement test

Note the human are similar in movements, and the vertical accelerations of human walking reduce after it increases. Therefore, there is no distinct difference in displacement for all people with different ages. Since the vertical accelerations of human walking depend on the changes of walking speed, in this section we focus on the accuracy test under different walking speed and walking distance.

4.1.1 Step accuracy: In this subsection, five testers were selected, who walk 50 steps randomly at slow, normal and fast speed, respectively. The number of steps of each walking was recorded in our system. As it is difficult to control the step rate accurately, there exist smaller differences at slow, normal and fast speed for different people. Note these differences have little influence on step accuracy, we do not record them in our results. The test results are shown in Table 2.

The test results show that: the accuracy rate of walking step count reaches up 100% at fast speed, while 98% at a normal speed. This is because that the lost step is smaller than in normal walking and fast walking when the vertical acceleration is relatively small at a slow step. It can be seen from Table 2, the differences of our approach are very small for different people. Our approach is more accurate than the previous work, only with 6% error.

4.1.2 Walking distance accuracy: In this subsection, five testers were selected, who walk 30 m at normal speed, fast speed, and fast speed. We recorded two results per walking. The test results are shown in Table 3.

Test results demonstrate that different people have various calculation displacements. This is because that the simplified calculation method is exploited based on the accelerations. Since the step size is related to leg length, walking speed and so on, there is litter individual difference for each person. The results manifest that it is more accurate at normal speed than at the slow and fast walking speed to calculate displacements. The main error in the slow walking is the steps will be lost, while the main error in the fast walking is not accurate enough. In the above experiment, the maximum error is only 6%, which has a high positioning accuracy.

Table 3 Test results of walking distance under different walking speed

Conner	Number	Distance/m	Low speed	Normal speed	High speed
A	1	30	28.272	28.980	28.545
	2	30	28.346	29.125	28.438
B	1	30	29.237	29.641	29.254
	2	30	29.368	29.673	29.242
C	1	30	28.542	28.870	29.307
	2	30	28.605	28.854	29.263
D	1	30	29.574	30.223	29.876
	2	30	29.659	30.562	29.980
E	1	30	29.410	29.796	29.351
	2	30	29.482	29.638	29.512

4.2 Walking direction

In this section, we focus on the test in the direction change of 90°, which are the common direction changes of people in walking.

4.2.1 Right angle turning: The testers are wearing this equipment, in a spacious indoor environment. They walk every five steps to turn to 90°, and last 10 times. The whole curves of this process are shown in Fig. 7 using MATLAB.

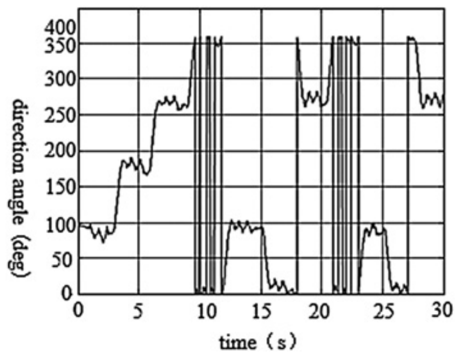

Fig. 7 *Test results of Quarter turn*

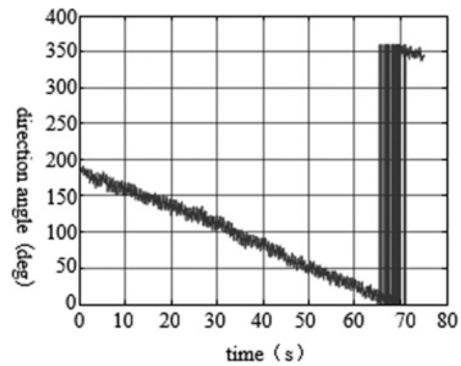

Fig. 8 *Test results of Bend walking*

Fig. 9 *Real walking track*

Fig. 10 *Track of System displaying*

It is seen from Fig. 7, there is 10 angles of 90°. The jump from 360° to 0° is because there is a slight fluctuation for the angle. It can be seen from the figure, the angle fluctuates even in straight. This is due to the swing of people in walking. With the averaging value of this period, we can get the current azimuth.

4.2.2 Bend walking: The tester embedded into devices, walk along the half circular track in the playground. The whole output of the system are as shown in Fig. 8 using MATLAB.

It is seen that from Fig. 8, the directions of walking in the test change from 180° to 350° roughly, with 190° errors.

4.3 Location test

To evaluate the effect of our system on localisation, a series of experiments have been conducted. We list a typical test in the first floor of a large shopping mall in Wuhan to demonstrate the effectiveness of the system. The planar graph of this shopping is shown in Fig. 9, denoted with white lines. The true trajectories are shown in Fig. 9, while the approximate trajectories from our system are shown in Fig. 10, denoted with black lines.

It is clear to see that there are some errors from Figs. 9 and 10, but there is not distinct difference between the location determined by WILA and the true locations. WILA can make the location more accurate if it can be modified with the map matching technique.

5 Conclusion

In this paper, a wearable indoor localisation approach is proposed to improve the localisation accuracy of previous work on wearable localisation. In the proposed approach, the wearable devices embedded into person are used to realise their displacement vectors, thus estimating their own locations. In addition, a walking prediction mechanism that predicts the moving direction of nodes is proposed to increase localisation accuracy. WILA is a scalable, practical and efficient localisation approach for IoT in mobile environments. The real-world experiment results demonstrate that our proposed approach achieves lower localisation error in various moving speeds.

6 Acknowledgment

This work has been partially supported by the National Basic Research Program of China (No. 2012CB315801), the National Natural Science Foundation of China (No. 61402343), and the EU FP7 CLIMBER Project (No. PIRSESGA-2012-318939).

7 References

1 Zhang, S., Liu, X., Wang, J., *et al.*: 'Accurate range-free localization for anisotropic wireless sensor networks:', *ACM Trans. Sensor Netw.*, 2015, **11**, (3), pp. 1–28

2 Wu, G., Wang, S., Wang, B., *et al.*: 'A novel range-free localization based on regulated neighborhood distance for wireless *Ad hoc* and sensor networks', *Comput. Netw.*, 2012, **56**, (16), pp. 3581–3593

3 Mao, G., Fidan, B., Anderson, B.D.: 'Wireless sensor network localization techniques', *Comput. Netw.*, 2007, **51**, (10), pp. 2529–2553

4 Savvides, A., Han, C.-C., Strivastava, M.B.: 'Dynamic fine-grained localization in ad-hoc networks of sensors'. Proc. IEEE MobiCom'01, Rome, Italy, 2001, pp. 166–179

5 Ayllón, D., Sánchez-Hevia, H.A., Gil-Pita, R., *et al.*: 'Indoor blind localization of smartphones by means of sensor data fusion', *IEEE Trans. Instrum. Meas.*, 2016, **65**, (4), pp. 783–794

6 Moreno, V., Zamora, M.A., Skarmeta, A.F.: 'A low-cost indoor localization system for energy sustainability in smart buildings', *IEEE Sens. J.*, 2016, **16**, (9), pp. 3246–3262

7 Collotta, M., Lo Cascio, A., Pau, G., *et al.*: 'Smart localization platform for IEEE 802.11 industrial networks'. Proc. SIES'13, Porto, 2013, pp. 69–72

8 Haddad, D.B., Martins, W.A., da Costa, M.d. V.M., *et al.*: 'Robust acoustic self-localization of mobile devices', *IEEE Trans. Mob. Comput.*, 2016, **15**, (4), pp. 982–995

9 Patwari, N., Ash, J.N., Kyperountas, S., *et al.*: 'Locating the nodes: cooperative localization in wireless sensor networks', *IEEE Signal Process. Mag.*, 2005, **22**, (4), pp. 54–69

10 Wymeersch, H., Lien, J., Win, M.Z.: 'Cooperative localization in wireless networks', *Proc. IEEE*, 2009, **97**, (2), pp. 427–450

11 Zickler, S., Veloso, M.: 'RSS-based relative localization and tethering for moving robots in unknown environments'. Proc. Robot'10, May 2010, pp. 5466–5471

12 Biswas Veloso, M.: 'WiFi localization and navigation for autonomous indoor mobile robots'. Proc. IEEE Robot'10, 2010, pp. 4379–4384

13 Caruso, A., Chessa, S., De, S., *et al.*: 'GPS-free coordinate assignment and routing in wireless sensor networks'. Proc. IEEE INFOCOM'05, Miami, USA, 2005, pp. 150–160

14 Niculescu, D., Nath, B.: '*Ad hoc* positioning system (APS) using AoA'. Proc. IEEE INFOCOM'03, 2003, pp. 1734–1743

15 Ho, C.C., Lee, R.: 'Real-time indoor positioning system based on RFID Heron-bilateration location estimation and IMU inertial-navigation location estimation'. Proc. COMPSAC'15, 2015, vol. 3, pp. 481–486

16 You, Y., Cha, H.: 'Scalable and low-cost acoustic source localization for wireless sensor network'. Proc. UIC '06, 2006, pp. 517–526

17 Zhang, J., Yan, T., Stankovi, J. A., *et al.*: 'Thunder: towards practical, zero cost acoustic localization for outdoor wireless sensor networks', *ACM Mob. Comput. Commun. Rev.*, 2007, **11**, (1), pp. 15–28

18 Nagpal, R., Shrobe, H., Bachrach, J.: 'Organizing a global coordinate system from local information on an *Ad Hoc* sensor network'. Proc. IPSN'03, 2003, pp. 333–348

19 He, T., Huang, C., Blum, B.M., *et al.*: 'Range-free localization schemes for large scale sensor networks'. Proc. MobiCom'03, 2003, pp. 81–95

20 Guha, S., Murty, R., Sirer, E.: 'Sextant: a unified node and event localization framework using non-convex constraints'. Proc. ACM MobiHoc'05, 2005, pp. 205–216

21 Kuśy, B., Ľedeczi, A., Maŕoti, M., *et al.*: 'Node density independent localization'. Proc IPSN'06, 2006, pp. 441–448

22 Xiao, Q., Xiao, B., Cao, J., *et al.*: 'Multihop range-free localization in anisotropic wireless sensor networks: A pattern-driven scheme', *IEEE Trans. Mob. Comput.*, 2010, **9**, (11), pp. 1592–1617

23 Sheu, J., Hu, W., Lin, J.: 'Distributed localization scheme for mobile sensor networks', *IEEE Trans. Mob. Comput.*, 2010, **9**, (4), pp. 516–526